

# Geophysical Research Letters®



## RESEARCH LETTER

10.1029/2024GL111497

## Asynchronous Poleward Migration of the Atlantic Subtropical Gyres Over the Past 22,000 years

### Key Points:

- Atlantic subtropical gyres have asynchronously migrated poleward over the last 22,000 years
- Poleward migration of the Atlantic subtropical gyres started ~1,500 years earlier in the Southern Hemisphere
- The northern boundary of North Atlantic subtropical gyre likely moved poleward at least 6°

Tainã M. L. Pinho<sup>1</sup> , Hu Yang<sup>1,2</sup> , Gerrit Lohmann<sup>1,3</sup> , Rodrigo C. Portilho-Ramos<sup>3</sup>, Cristiano M. Chiessi<sup>4</sup> , Andre Bahr<sup>5</sup> , Dirk Nürnberg<sup>6</sup> , Janne Repschläger<sup>7</sup>, Xiaoxu Shi<sup>1</sup>, Ralf Tiedemann<sup>1</sup>, and Stefan Mulitza<sup>3</sup> 

<sup>1</sup>Alfred Wegener Institute for Polar and Marine Research, Bremerhaven, Germany, <sup>2</sup>Southern Marine Science and Engineering Guangdong Laboratory, Zhuhai, China, <sup>3</sup>MARUM—Center for Marine Environmental Sciences, University of Bremen, Bremen, Germany, <sup>4</sup>School of Arts, Sciences and Humanities, University of São Paulo, São Paulo, Brazil, <sup>5</sup>Institute of Earth Sciences, Heidelberg University, Heidelberg, Germany, <sup>6</sup>GEOMAR Helmholtz Centre for Ocean Research Kiel, Kiel, Germany, <sup>7</sup>Department of Climate Geochemistry, Max Planck Institute for Chemistry, Mainz, Germany

### Supporting Information:

Supporting Information may be found in the online version of this article.

### Correspondence to:

T. M. L. Pinho and H. Yang,  
taina.pinho@awi.de;  
yanghu@sml-zhuhai.cn

### Citation:

Pinho, T. M. L., Yang, H., Lohmann, G., Portilho-Ramos, R. C., Chiessi, C. M., Bahr, A., et al. (2025). Asynchronous poleward migration of the Atlantic subtropical gyres over the past 22,000 years. *Geophysical Research Letters*, 52, e2024GL111497. <https://doi.org/10.1029/2024GL111497>

Received 23 JUL 2024  
Accepted 15 JAN 2025

**Abstract** By exchanging huge amounts of heat between the tropics and high latitudes, subtropical gyres significantly impact Earth's energy balance. Yet, their dynamical changes during the last deglaciation remain poorly understood. Here, nine records of the planktonic foraminiferal species *Globorotalia truncatulinoides*, that inhabits the permanent deep thermocline of subtropical gyres, are used to explore the meridional migration of both the North and South Atlantic subtropical gyres (NASG and SASG, respectively) in the past 22,000 years. We find that both gyres migrated poleward, with the SASG migration 1,500 years earlier than the NASG. Records from the North Atlantic Ocean indicate that the NASG's northern boundary has shifted over 6°. Climate model simulations suggest that these migrations are coupled with shifts in meridional temperature gradients. The poleward migration of the Atlantic subtropical gyres was crucial for sustaining a milder modern high-latitude climate in comparison with that of the last ice age.

**Plain Language Summary** Subtropical gyres are vast ocean circulation systems that transport upper ocean water between the tropics and high latitudes, that are vital for regulating Earth's climate. We studied how these gyres in the Atlantic Ocean changed during the last 22,000 years. By compiling microfossil records of a specific planktonic foraminifera species found in marine sediment cores near the boundary of subtropical gyres, we found that the Atlantic subtropical gyres migrated poleward since the last ice age. This poleward migration was gradual and lasted for a very long period from the last deglaciation throughout the Holocene. Some of the regional migrations reached an amplitude of more than 6°. Our study emphasizes the importance of gyre position in shaping the heat transport in the Atlantic Ocean. These results point to a natural long-distance migration in the gyres on glacial-interglacial timescale, implying a potentially dramatic migration influenced by anthropogenic activities.

## 1. Introduction

Subtropical gyres are large-scale anticyclonic ocean circulation induced by wind stress curl (Munk, 1950). They play a crucial role in transferring energy between tropical and midlatitude regions, thereby influencing the global climate system (Garzoli et al., 2013; Garzoli & Matano, 2011; Schmitz & McCartney, 1993; Schmitz & McCartney, 1993; Talley, 2003).

Understanding subtropical gyre changes is essential for fully assessing their impacts on human society and marine ecosystems. Satellite observations reveal that the Earth's major ocean gyres are drifting poleward at a rate of approximately 0.1° per decade, potentially reaching 1° in response to a doubling CO<sub>2</sub> (Yang, Lohmann, Krebs-Kanzow, et al., 2020). The drifted ocean gyres drive enhanced warming over the subtropical branches of the gyres, that is, western boundary currents (Wu et al., 2012; Yang et al., 2016), reshaping the distribution of marine ecosystem (Aquad & Martos, 2012; Gianelli et al., 2019; Pershing et al., 2015; Steinacher et al., 2010; Stramma et al., 2008). Migrations in subtropical gyres and subtropical fronts are closely coupled to the poleward movement of large-scale atmospheric circulation (Shaw, 2019), which in turn shifts dry climate zones poleward, affecting weather patterns in subtropical regions (Primeau & Cessi, 2001). Furthermore, changes in the subtropical gyres contribute to additional sea level rises relative to the global mean in subtropical regions (Yin & Goddard, 2013).

© 2025. The Author(s).

This is an open access article under the terms of the [Creative Commons Attribution License](https://creativecommons.org/licenses/by/4.0/), which permits use, distribution and reproduction in any medium, provided the original work is properly cited.

Interestingly, the meridional migration of oceanic features is recorded not only by satellites but also by marine sediment cores (Bard & Rickaby, 2009; Gray et al., 2020; Yang, Lohmann, Krebs-Kanzow, et al., 2020). Palaeoceanographic reconstructions show meridional fluctuations in the subtropical fronts (Bard & Rickaby, 2009; Barker & Diz, 2014; Barker et al., 2009; Dyez et al., 2014; Peeters et al., 2004), which define the midlatitude boundaries of subtropical gyres. Contemporary observations show only minor poleward migrations, but marine sediment cores, such as those from the Pacific and Indian Oceans, suggest drastic shifts of 3–7° during glacial-interglacial transitions (Ai et al., 2024; Bard & Rickaby, 2009; Gray et al., 2020). These findings highlight the sensitivity of subtropical fronts to natural climate variability in the past. Nonetheless, substantial gaps persist in understanding long-term changes in the geometry and dynamics of the entire subtropical gyres across different climatic conditions (e.g., Pinho et al., 2021). For instance, evidences suggest a meridional contraction of the SASG under full glacial boundary conditions rather than a mere northward shift, when only the subtropical front is examined (Pinho et al., 2021).

In this study, we examine the meridional migration of the Atlantic subtropical gyres since the last 22,000 years by integrating paleo-proxy information from marine sediment cores and climate model simulations. We analyze cores from both the northern and southern boundaries of the Atlantic subtropical gyres to provide a comprehensive interpretation of the Atlantic gyre system (Figure 1). This method accounts for both meridional shifts and potential contractions and expansions of the gyre.

## 2. Data and Methods

### 2.1. *Globorotalia truncatulinoides* as Proxy for the Meridional Displacement of the Atlantic Subtropical Gyres

Planktonic foraminifera *Globorotalia truncatulinoides* reproduces in shallow waters, but grows and calcifies while sinking down to a few hundred meters water depth in a one-year cycle (Lohmann & Schweitzer, 1990; Mulitza et al., 1997). Therefore, *G. truncatulinoides* is remarkably dependent on deep-reaching ventilated warm waters (Lohmann & Schweitzer, 1990; Mulitza et al., 1997), which can only be found in subtropical gyres due to the dominant convergence and downwelling (Figure 1b). *G. truncatulinoides* increases in abundance at the center of subtropical gyres, where warm water reaches the deepest depths (Lohmann & Schweitzer, 1990; Mulitza et al., 1997) (Figures 1a and 1c). In contrast, *G. truncatulinoides* decreases in abundance at the boundary of subtropical gyres where warm water reaches the shallowest depths (Lohmann & Schweitzer, 1990; Mulitza et al., 1997) (Figure 1a). This is related to changes in the upper water column stratification. We are using both dextral and sinistral morphotypes as the most accurate representation of physical oceanographic conditions for the subtropical gyre circulation is achieved when they are considered together (Figures 1a and 1b) (also Pinho et al., 2021).

We compiled records of *G. truncatulinoides* from nine marine sediment cores distributed across the North and South Atlantic (Figure 1a and Table S1 in Supporting Information S1). In the North Atlantic, six cores were selected, spanning a latitudinal range from 12.09°N to 44.36°N, while in the South Atlantic, three cores were chosen, ranging from 10.94°S to 44.15°S (Figure 1a and Table S1 in Supporting Information S1). These records were strategically located at the northern and southern boundaries of the North Atlantic subtropical gyre (NASG) and South Atlantic subtropical gyre (SASG).

*Globorotalia truncatulinoides* comprise a complex of four to five species, as revealed by genetic and morphometric analyses (de Vargas et al., 2001; Quillévéré et al., 2013; Ujjié et al., 2010). Importantly, no significant differences in the abundance of sinistral and dextral morphotypes were observed over the past 22 ka in the records analyzed herein. Regardless of the genotypes of *G. truncatulinoides* (De Vargas et al., 2001) present in our records, upper water column stratification likely remains the key factor for controlling their proliferation at the NASG and SASG meridional boundaries (Figures 1a–1c, see also Figure 1 of Pinho et al., 2021). Further in-depth details on the morphotypes and genotypes are presented in Supporting Information S1.

### 2.2. Model Simulations

To investigate the physical processes responsible for dynamical changes of the NASG and SASG, we compared the proxy results with climate model simulations performed with the state-of-the-art Alfred Wegener Institute Earth System Model (AWI-ESM, Sidorenko et al., 2019). First, two time-slice simulations covering the LGM

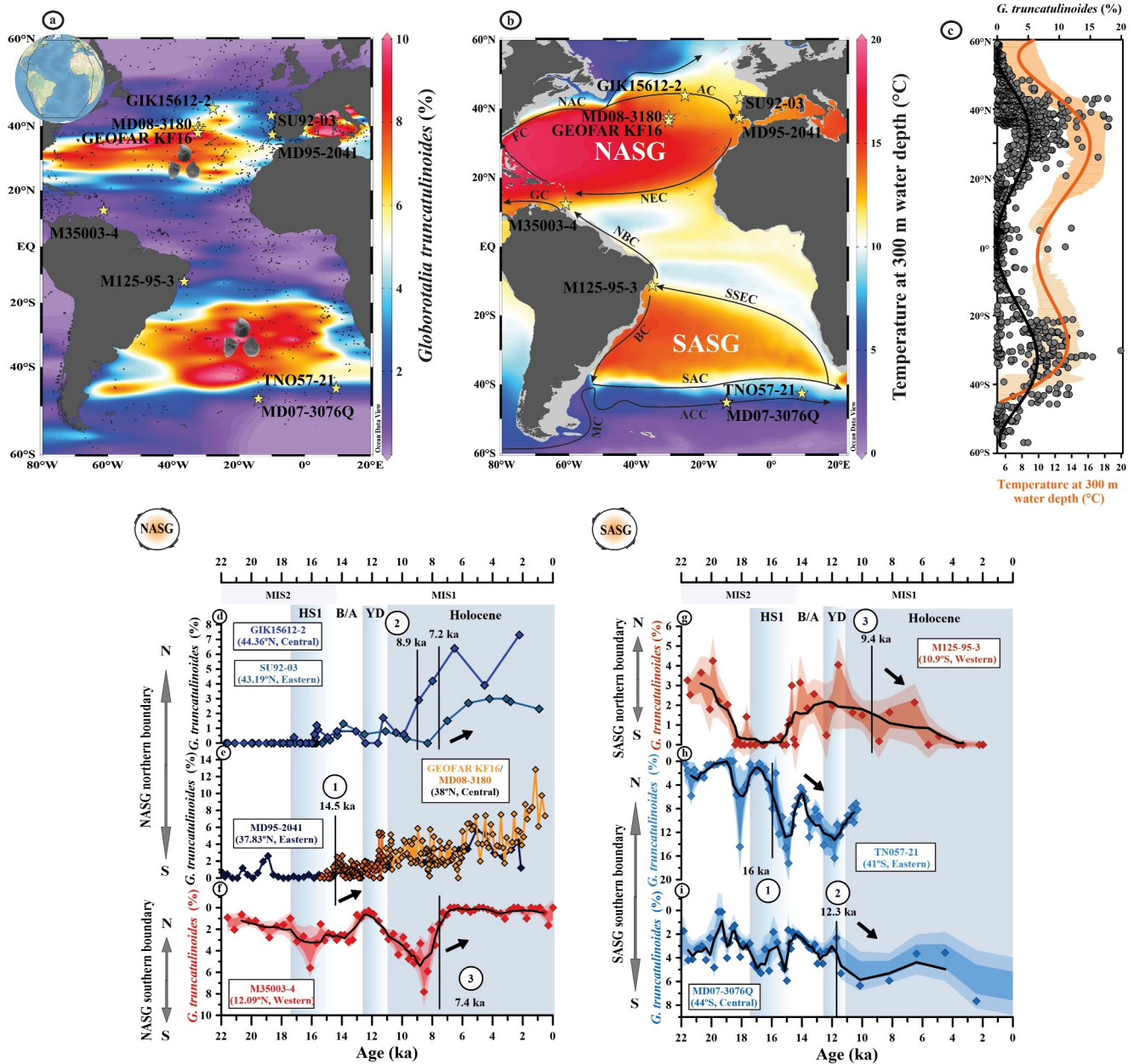


**Figure 1.** Location of the investigated marine sediment cores (yellow stars) in relation to the North and South Atlantic subtropical gyres (NASG and SASG, respectively) and their relative abundances of *Globorotalia truncatulinoides* covering the last 22,000 years. (a) Modern distribution of planktonic foraminifera *Globorotalia truncatulinoides* in the Atlantic Ocean (ForCenS) (Siccha & Kucera, 2017a, 2017b), black dots depict the sites of the surface sediment samples (see more details in Supporting Information S1). (b) Annual mean subsurface (i.e., 300 m water depth) temperature (Locarnini et al., 2019). Black arrows represent the main surface ocean currents (Lherminier et al., 2010; Schott et al., 2004; Stramma & England, 1999). Antarctic Circumpolar Current (ACC), Azores Current (AC), Brazil Current (BC), Guinea Current (GC), Florida Current (FC), Malvinas Current (MC), North Atlantic Current (NAC), North Brazil Current (NBC), North Equatorial Current (NEC), South Atlantic Current (SAC), and Southern South Equatorial Current (SSEC). (c) Atlantic zonal mean annual subsurface temperature (i.e., 300 m water depth) (Locarnini et al., 2019; orange line represents a polynomial fit) and modern distribution of *G. truncatulinoides* (black line represents a polynomial fit). (d) Relative abundance of *G. truncatulinoides* from cores; GIK1562-2 (Kiefer, 1998), and SU92-03 (Salgueiro et al., 2010), (e) GEOFAR KF16, MD08-3180 (Repschläger et al., 2015, 2023), and MD95-2041 (Voelker, 2010), (f) M35003-4 (Hüls & Zahn, 2000), (g) M125-95-3 (Pinho et al., 2021), (h) TNO57-21 (Barker et al., 2009), and (i) MD07-3076Q (Gottschalk et al., 2015). Marine Isotope Stages (MIS), are shown below the upper horizontal axis. Heinrich Stadial 1 (HS1) and Younger Dryas (YD) are represented by light blue vertical bars. We smoothed curves using five point running average in panels (f)–(i) and three point running average in panel (i). Vertical dashed lines indicate the point from which *G. truncatulinoides* continually increases in subtropical boundaries and decreases in tropical boundaries of NASG and SASG on a long-term timescale basis (see more details in Supporting Information S1, Table S2 and Figure S3 in Supporting Information S1). Numbers 1, 2, and 3 in all panels represent the chronological order of poleward shifts for each boundary of NASG and SASG. Shading colors indicate 1 and 2-σ confidence envelopes in panels (f)–(i). Note that y-axes of panels (c), (e), and (f) are inverted in order to give a more intuitive information regarding the meridional displacements.

(~21 kyr Before Present, hereafter, ka) and the pre-industrial periods were conducted. These two experiments were designed according to the protocol of Paleoclimate Modelling Intercomparison Project–Phase 4 (PMIP4, Kageyama et al., 2017). They are used to examine the long-term changes of the NASG and SASG during the LGM and Pre-industrial to present. Detailed information of the model resolution and setup can also be found in Shi et al. (2020, 2023).

Additionally, a freshwater perturbation experiment is performed to examine the NASG and SASG evolution associated with millennial-scale variability of the Atlantic Meridional Overturning Circulation (AMOC) during the deglaciation. The freshwater perturbation experiment is performed by applying an 0.1 Sverdrup (Sv) freshwater input over the North Atlantic subpolar ocean (50–60°N) under the LGM background climate. In our simulation, the AMOC weakens significantly from a value of ~18 Sv to ~8 Sv after 200 years freshwater perturbation, causing widespread cooling over the Northern Hemisphere (Figures S1 and S2 in Supporting Information S1). The freshwater perturbation simulates past freshwater discharge events that weakened ocean heat transport broader cooling over the Northern Hemisphere, and warming over the Southern Hemisphere (Heinrich, 1988; Rainsley et al., 2018).

### 3. Long-Term Poleward Migration of the Atlantic Subtropical Gyres Since the Last Glacial Maximum

#### 3.1. Migration of the North Atlantic Subtropical Gyre

The abundance of *G. truncatulinoides* displays an overall positive trend at the northern boundary of NASG (nNASG) over the past 22 ka (Figures 1d and 1e), suggesting a poleward migration of nNASG. During the interval of 22–18 ka, the absence of *G. truncatulinoides* in cores GIK15612-2 (Kiefer, 1998), SU92-03 (Salgueiro et al., 2010), together with its presence in core MD95-2041 (Voelker, 2010) at ~1.5%, indicates that the nNASG was situated between 37.83°N and 43.19°N (Figures 1d and 1e). During Heinrich Stadial 1 (HS1, ~18–15 ka), nearly absence of the *G. truncatulinoides* in cores MD95-2041 and GEOFAR KF16 indicates that the nNASG was around 38°N. This represents a southernmost position of the nNASG (Figures 1a, 1b, and 1d). The systematic poleward shift of the nNASG started during the Bølling-Allerød (B/A) event at ~14.5 ka and continued throughout the Holocene, as given by the overall increase in *G. truncatulinoides* in cores GEOFAR KF16, MD08-3180, and MD95-2041 (Repschläger et al., 2015, 2023; Voelker, 2010) (Figure 1e), collected at ~38°N. This poleward shift of the nNASG is briefly interrupted by a relatively stable dynamic during the Younger Dryas (YD). A similar northward shift is observed at higher latitudes in the North Atlantic from 43.19°N to 44.36°N, but with a delay of ~6.5 kyr (i.e., from 8.89 to 7.25 ka) (Figure 1e). This suggests that the nNASG shifted 5–6° to the north within ~6.5 kyr. During the Holocene, *G. truncatulinoides* kept increasing in cores GIK15612-2 and SU92-03, suggesting that the nNASG continued to move poleward.

In the tropical North Atlantic, the increases in *G. truncatulinoides* abundance observed in core M35003-4 (Hüls & Zahn, 2000) within the southern boundary of the NASG (sNASG) briefly during HS1 and more sustained from 11.5 to 7.4 ka suggests southward displacements of the sNASG during the deglaciation and early Holocene. Combining the increases in *G. truncatulinoides* in the nNASG, this suggests that the entire NASG may have undergone a meridional expansion from 11.5 to 7.4 ka (Figure 1f). Subsequently, *G. truncatulinoides* in core M35003-4 declines to the present days, indicating a poleward shift of the sNASG (Figure 1f).

Thus, considering both the nNASG and sNASG together, we found that the NASG completed its poleward migration, involving a concurrent poleward shift of the nNASG and sNASG, only after the early Holocene (Figures 1d–1f). We suggest that the poleward shift of the nNASG initially begins around 38°N. Subsequently, the sNASG initiates a poleward shift in the tropical North Atlantic within the early Holocene (Figures 1d–1f).

#### 3.2. Migration of the South Atlantic Subtropical Gyre

During the LGM, full glacial conditions forced the southern boundary of the SASG (sSASG) to shift northward, restricting its poleward shifts until the deglacial period (Pinho et al., 2021). Over the South Atlantic, a long-standing 8% increase in *G. truncatulinoides* is observed in core TN057-21 (Barker et al., 2009) (Figure 1h), located within the sSASG at ~41°S spanning from 16 ka (i.e., HS1) to the Holocene. This indicates a poleward displacement of the sSASG. Interestingly, the timing parallels that documented in the subtropical boundary of the North Pacific subpolar gyre (Gray et al., 2020). The *G. truncatulinoides* record from core MD07-3076Q

(Gottschalk et al., 2015), located further south at about 44°S, also depicts increases, albeit ~3.6 kyr later. The delayed responses exhibit similar patterns regarding the initial movement of the subtropical boundaries of both the NASG and SASG (Figures 1d, 1e, 1h, and 1i). Longer delayed response observed at the nNASG compared to the sSASG can be attributed to the greater distance between cores, which is twice as high in the nNASG (i.e., a difference of 6° latitude). The rate of poleward shift of nNASG and sSASG is respectively 0.83°/kyr and 0.84°/kyr (Supporting Information S1).

Considering the meridional baseline at 41°S (core TN057-21), we hypothesize a minimum 3° southward shift of the sSASG within 4 kyr over the last deglacial period. However, it is plausible that during the LGM, the sSASG was displaced north of 41°S (e.g., Jonkers et al., 2024). In agreement, a 4.8° southward shift of the Southern Hemisphere westerlies is documented over the last deglacial period (Gray et al., 2023). It is important to note that while the boundaries of the NASG and SASG may have exhibited different meridional patterns along their longitudinal extents, there is a lack of high-resolution *G. truncatulinoides* records available from different longitudes spanning a west-east transect for each gyre boundary since the LGM.

Similar to the sNASG, tracking meridional changes in the northern boundary of the SASG (nSASG) has been limited to one location, hindering our ability to determine the magnitude of meridional changes and timing in the tropical South Atlantic. In the nSASG, *G. truncatulinoides* shows a long-term increase in core M125-95-3 (Pinho et al., 2021) spanning from 16 to 10.6 ka (Figure 1g). This may suggest a meridional expansion of the SASG, akin to observations in the NASG, albeit occurring over a different interval (i.e., 16 to 10.6 ka) (Figure 1f). Finally, a long-term decrease in *G. truncatulinoides* in core M125-95-3 (Pinho et al., 2021) begins at ~10.6 ka and progresses throughout the Holocene. This decreasing pattern indicates a poleward shift of the nSASG (Figure 1g), marking the complete poleward migration of the SASG due to the concurrent poleward shift of both the nSASG and sSASG.

In both NASG and SASG, the poleward shift of gyres is first detected in lower latitudinal bands of the subtropical boundaries as suggested by our change-point analysis (see Supporting Information S1) (Figures 1d–1i, Figure S3 and Table S2 in Supporting Information S1). We found that the Atlantic gyres respond first in the Southern Hemisphere, as the systematic poleward shift of SASG begins ~1.5 kyr earlier than that seen in the NASG (Figures 1e and 1h).

#### 4. Migration of the Subtropical Gyres Simulated in Climate Model

In order to evaluate our proxy interpretation, we performed climate model simulations to reconstruct the climate states during the LGM, Pre-Industrial and millennial-scale weak AMOC, such as HS1. As illustrated in Figure 1b, the subtropical gyres are related to relatively warm subsurface water due to dominant downwelling. However, temperature change is not a reliable metric to infer gyre shifts because of the overall ocean warming from LGM to the present. Here, we use temperature gradients as an indirect metric to examine the gyre shifts, because the subtropical gyre boundaries are visible from relatively strong horizontal temperature gradients (Figure 2, dense contours).

As shown in Figure 2a, dipole modes of positive (negative) temperature gradient anomalies are found at the polar (equatorial) flanks of both the nNASG and sNASG. This suggests that the NASG is displaced more poleward during the Pre-industrial era compared with that of the LGM, consistent with the proxy data (Figures 1d–1f). Similar to the NASG, the poleward shift of the sSASG is observed in the model simulation (Figure 2a), manifesting positive (negative) temperature gradients at polar (equatorial) flanks of the sSASG. However, the shift in the nSASG is not evident.

In contrast to the poleward migration, the NASG and SASG show a southward migration in the freshwater perturbation experiment. This is evident by the negative/positive temperature gradient anomalies at the north/south flanks of the subtropical extension of the Gulf Stream and Brazil Current. The southward migration of the NASG is consistent with the reduction in *G. truncatulinoides* found in core MD95-2041 during HS1 (Figure 1e). Moreover, it also explains the early poleward/southward migration of the SASG, as revealed by the increase in *G. truncatulinoides* detected in core TN057-21 around 16 ka (Figure 1h).

Interestingly, the meridional migration of the subtropical gyres is not limited to the Atlantic Ocean, but also occurs in the North Pacific and Indian Oceans. For example, positive/negative temperature gradient anomalies are also found near the mid-latitude boundaries of North Pacific subtropical gyre (~40°N) and Indian Ocean (~40°S).

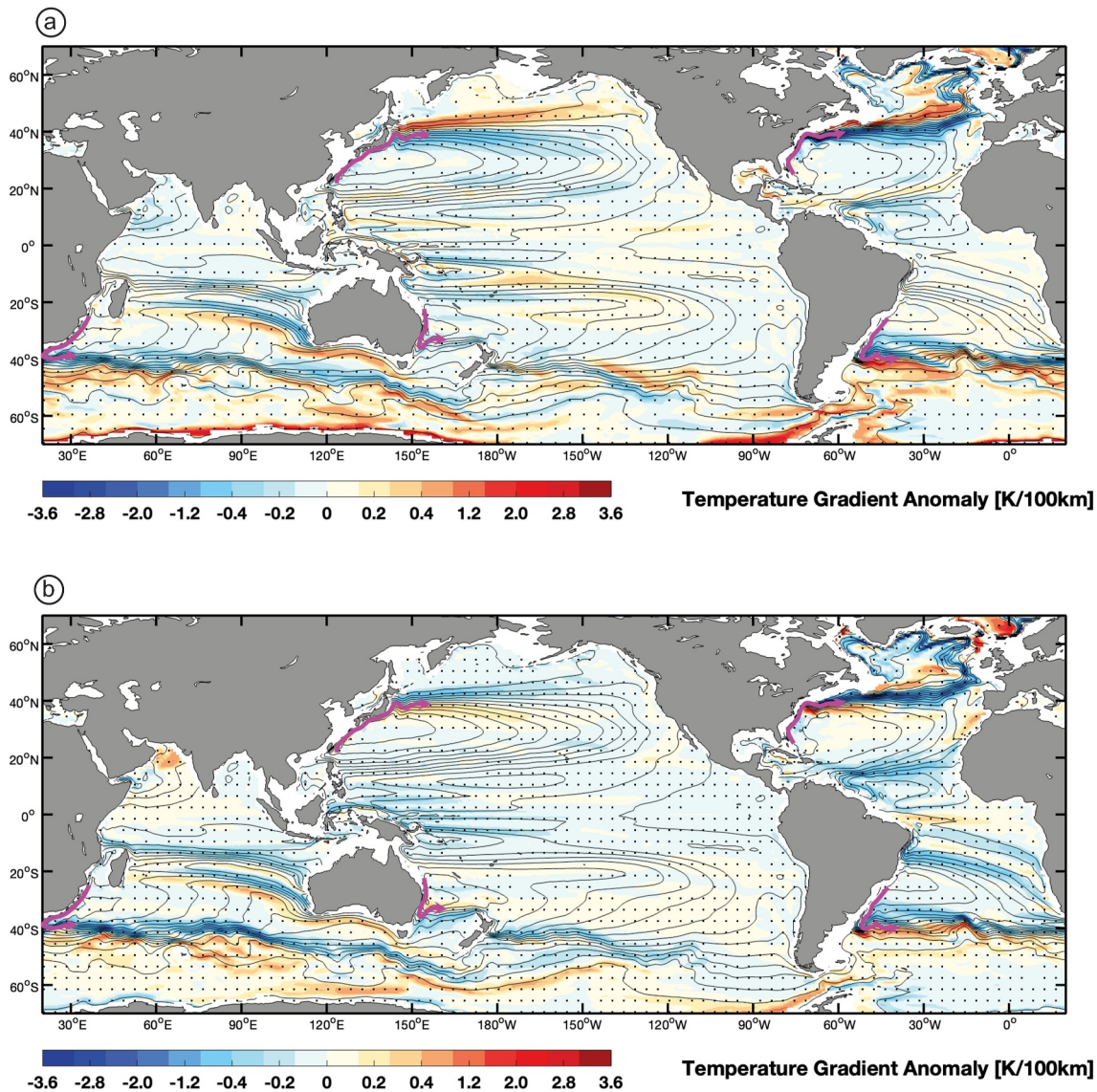


**Figure 2.** Simulated migration of subtropical gyres due to (a) deglacial warming and (b) AMOC weakening. The contour lines illustrate the annual mean subsurface temperature (i.e., 300 m water depth, cf. Figure 1b) in the Last Glacial Maximum (LGM) simulation. Due to dominant downwelling, the subsurface temperature is relatively high in the subtropical gyres, the boundaries of subtropical gyres are marked by strong temperature gradients (dense contour lines). The pink arrows illustrate the subtropical western boundary currents in the LGM experiment. The color shading represents subsurface (300 m water depth) horizontal temperature gradient anomalies in the (a) Pre-Industrial experiment and (b) freshwater perturbation experiment with respect to the LGM experiment. Positive/negative anomalies pattern at polar/equatorial flanks of subtropical gyre boundaries indicate a poleward migration of subtropical gyres. Stippling indicates regions where the anomalies are statistically significant (Student's *t*-test).

These migrations causes anomalously strong warming/cooling over the subtropical extensions of the Gulf Stream, Brazil Current, Kuroshio Current and Agulhas Current (Figures 3a and 3b) (Beech et al., 2022; Li et al., 2022; Wu et al., 2012; Yang et al., 2016). In contrast, the migration in the Eastern Australian Current is likely not as pronounced.

### 5. Mechanism

Modern observations and simulations indicate a poleward shift of oceanic and atmospheric circulation under a warming climate (Shaw, 2019; Yang, Lohmann, Krebs-Kanzow, et al., 2020). Previous studies proposed that an initial migration in the meridional temperature gradients thermodynamically drives a shift in atmospheric circulation, whereas the shift in atmospheric circulation, specifically winds, dynamically forces the shift in oceanic

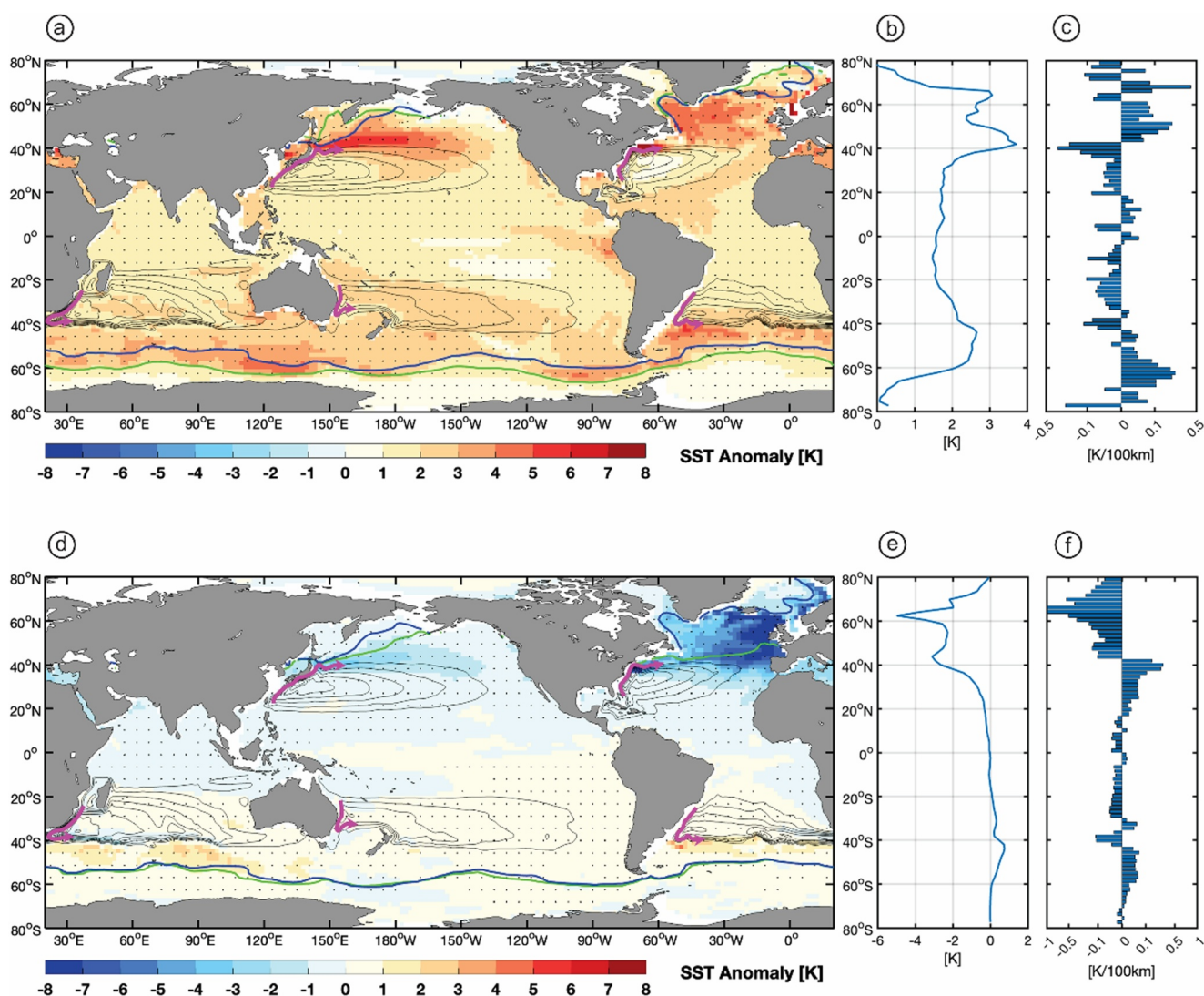


**Figure 3.** Simulated ocean temperature anomalies and meridional shift of the meridional sea surface temperature gradients. (a) Sea surface temperature anomaly: Pre-industrial minus Last Glacial Maximum (LGM). (b) Zonal mean SST anomaly. (c) Zonal mean meridional temperature gradient anomaly, indicating a poleward shift of the temperature gradients. Stippling indicates regions where the anomalies are statistically significant (Student's *t*-test). (d–f) Contours show the barotropic stream function of the subtropical gyres in the LGM. The pink arrows illustrate the subtropical western boundary currents. The blue and green lines illustrate the sea ice edge (10% annual mean sea ice concentration) in LGM and Pre-industrial, respectively.

circulation (Yang, Lohmann, Lu, et al., 2020; Yang et al., 2022). To explore the potential mechanism of gyre migration since the LGM, we examined the ocean warming pattern and related anomalies in meridional temperature gradient in the Pre-industrial and freshwater perturbation experiments with regard to the LGM.

As shown in Figure 3a, the Pre-industrial climate is significantly warmer than the LGM, with a retreat of polar sea ice and a spatially heterogeneous warming trend. According to the physical laws governing temperature changes, such as the Clausius-Clapeyron relation and the Stefan-Boltzmann law, temperature bears a nonlinear relationship with radiation and saturated vapor pressure. The same increases in sea surface temperature in tropical areas are more difficult than those in mid-high latitudes as they cause more upward radiation and evaporation. As a result, the temperature rises in the tropical area are minor, leading to a flatter meridional temperature gradient at low-latitudes (Figures 3b and 3c, 0°–40°). In contrast, at higher latitudes, the presence of sea ice limits the rise in water temperature close to the sea ice margin. Further away from the sea ice edge, the subpolar ocean experiences strong warming, resulting in an increase in meridional temperature gradient at higher latitudes (Figures 3b and 3c, 45°–70°). Ultimately, the overall meridional temperature gradients shift to higher latitudes, driving a

corresponding migration in the oceanic and atmospheric circulation. This long-term poleward shift is likely primarily driven by rising CO<sub>2</sub> from LGM to present (Kohler et al., 2017), as Earth's orbit changes between the LGM and present are relatively minor (Berger, 1978; Shi et al., 2023).

Besides the long-term poleward shift of the Atlantic subtropical gyres, we also identified millennial-scale migrations. These shifts are likely attributed to the millennial-scale changes in the AMOC strength. As shown in Figure 3d, during a weakened AMOC state, a shallow mixed layer (due to a fresher upper ocean) of the North Atlantic subpolar ocean promotes more sea ice coverage. This results in the expansion of polar water and the migration of the meridional temperature gradient toward lower latitudes (Figures 3e and 3f). Distinctly from the North Atlantic, the South Atlantic exhibits an opposite thermal response (Crowley, 1992; Santos et al., 2022; Stocker & Johnsen, 2003), which migrates the meridional temperature gradients toward high southern latitudes (Figure 3f). This migration thermally drives shifts in winds, whereas changes in atmospheric winds dynamically drive shifts in ocean gyres (Yang et al., 2022). In this context, the collapse of the AMOC during HS1 caused the early poleward/southward migration of the SASG (Pinho et al., 2021). In contrast, the resumption of the AMOC during the B/A drives North Atlantic warming and poleward/northward migration of the NASG a few thousand years later (Crowley, 1992; Pedro et al., 2018; Stocker & Johnsen, 2003). The poleward shift of the SASG starts midway through HS1 (~16 ka), while poleward shift of the NASG begins at the onset of the B/A (~14.5 ka). This 1.5 kyr lag suggests that AMOC-induced changes cause asynchronous poleward shift responses between the NASG and the SASG. A pronounced initial equatorward position of the nNASG and the sSASG during the LGM should set their meridional starting points, explaining why the subsequent poleward shifts start from lower latitudinal bands of the subtropical boundaries.

## 6. Discussion and Conclusions

Subtropical gyres are a key component of the ocean circulation system, connecting the tropics to the mid-latitudes regions. Modern observations reveal that subtropical gyres have moved toward higher latitudes over the past four decades (Yang, Lohmann, Krebs-Kanzow, et al., 2020). However, tracking their long-term changes is challenging, particularly on orbital timescale. Here, we investigate a collection of the relative abundance of *G. truncatulinoides* records from nine marine sediment cores located at the northern and southern boundaries of the Atlantic subtropical gyres over the last 22 kyr. Accounting for these complex species, existing mainly in subtropical gyres, may provide an ideal way to identify the meridional movement of subtropical gyres. Our results suggest that both the NASG and SASG have experienced long periods of migration toward higher latitudes since the LGM. Regional migration reached an amplitude of 6°, much larger than what has been indicated in modern observations. Such large migrations were detected not only in the Atlantic Ocean, but also in the Pacific (Gray et al., 2020) and Indian (Ai et al., 2024; Bard & Rickaby, 2009) Oceans in the past glacial-interglacial cycles.

We recognize that the long-term poleward migration is marked by several millennial-scale variations, especially during the last deglaciation (Figures 1d–1i). These variations are likely linked to millennial-scale changes in AMOC strength. Previous studies based on various (paleo) proxies have suggested a southward displacement of the NASG (Calvo et al., 2001; Reißig et al., 2019; Repschläger et al., 2015; Schiebel et al., 2002) during periods of abrupt AMOC slowdown, such as the HS1 and the YD (Lippold et al., 2016; McManus et al., 2004). A southward shift of the SASG has also been documented and is thought to have contributed to the rise in atmospheric CO<sub>2</sub> during HS (Pinho et al., 2021). We found an earlier poleward shift response of the SASG compared to the NASG, likely due to the AMOC-induced interhemispheric gradients.

An earlier study suggests that the migration in ocean circulation is closely coupled with atmosphere circulation (Yang, Lohmann, Krebs-Kanzow, et al., 2020). The identified migration of the Atlantic gyres, therefore, can be seen as a manifestation of a poleward shift in large-scale oceanic and atmospheric circulations, affecting most of the global climate zones. Our micropaleontological records reveal a long-term poleward migration of the subtropical Atlantic gyres, indicating a consistent signal of natural climate variability since the transient warming of the last deglaciation, which is aligned with our model simulation.

As the subtropical gyres transport large amount of heat toward high latitudes, a poleward migration of these gyres allows low-latitude warm waters to reach higher latitudes and help to maintain a relatively warm high-latitude present climate in comparison with the LGM. Yet, further poleward migration contributes to an amplified ocean warming in the Arctic (Shu et al., 2022; Wang et al., 2024).



## Data Availability Statement

The compiled data used here can be found in the original publications (Barker et al., 2009; Gottschalk et al., 2015; Hüls & Zahn, 2000; Kiefer, 1998; Pinho et al., 2021; Repschläger et al., 2015, 2023; Salgueiro et al., 2010; Voelker, 2010) as shown in Table S1 in Supporting Information S1. The AWI-ESM model code is publicly available at <https://www.fesom.de/models/awi-esm>. Modern foraminiferal data used here are available from the World Data Center PANGAEA (ForCenS) (Siccha & Kucera, 2017b).

## Acknowledgments

T.M.L.P. acknowledges the support from INSPIRES project and Open Access publication fund of Alfred-Wegener-Institut Helmholtz-Zentrum für Polar- und Meeresforschung. H.Y. acknowledges the support from the construction fund of the Frontier Research Center at the Southern Marine Science and Engineering Guangdong Laboratory (Zhuhai), No. SML2023SP204, the Ocean Negative Carbon Emissions (ONCE) Program and the National Natural Science Foundation of China. G.L. acknowledges support by Bundesministerium für Bildung und Forschung via REKLIM, PalMod, and the research program “Changing Earth—Sustaining our Future.” R.C.P.R. acknowledges the support from Cluster of Excellence “The Ocean Floor—Earth’s Uncharted Interface” (EXC-2077, Project 390741603). This study was financed, in part, by the São Paulo Research Foundation (FAPESP), Brazil, processes number 2018/15123-4 and 2019/24349-9. C.M.C. acknowledges the financial support from CNPq (Grant 312458/2020-7) and CAPES\_COFECUB (Grants 8881.712022/2022-1 and 49558SM). Open Access funding enabled and organized by Projekt DEAL.

## References

- Ai, X. E., Thöle, L. M., Auderset, A., Schmitt, M., Moretti, S., Studer, A. S., et al. (2024). The southward migration of the Antarctic Circumpolar Current enhanced oceanic degassing of carbon dioxide during the last two deglaciations. *Communications Earth & Environment*, 5(1), 58. <https://doi.org/10.1038/s43247-024-01216-x>
- Auad, G., & Martos, P. (2012). Climate variability of the northern Argentinean shelf circulation: Impact on *Engraulis Anchoita*. *The International Journal of Ocean and Climate Systems*, 3(1), 17–43. <https://doi.org/10.1260/1759-3131.3.1.17>
- Bard, E., & Rickaby, R. E. M. (2009). Migration of the subtropical front as a modulator of glacial climate. *Nature*, 460(7253), 380–383. <https://doi.org/10.1038/nature08189>
- Barker, S., & Diz, P. (2014). Timing of the descent into the last Ice Age determined by the bipolar seesaw. *Paleoceanography*, 29(6), 489–507. <https://doi.org/10.1002/2014PA002623>
- Barker, S., Diz, P., Vautravers, M. J., Pike, J., Knorr, G., Hall, I. R., & Broecker, W. S. (2009). Interhemispheric Atlantic seesaw response during the last deglaciation. *Nature*, 457(7233), 1097–1102. <https://doi.org/10.1038/nature07770>
- Beech, N., Rackow, T., Semmler, T., Danilov, S., Wang, Q., & Jung, T. (2022). Long-term evolution of ocean eddy activity in a warming world. *Nature Climate Change*, 12(10), 910–917. <https://doi.org/10.1038/s41558-022-01478-3>
- Berger, A. (1978). Long-term variations of daily insolation and quaternary climatic changes. *Journal of the Atmospheric Sciences*, 35(12), 2362–2367. [https://doi.org/10.1175/1520-0469\(1978\)035<2362:LTVODI>2.0.CO;2](https://doi.org/10.1175/1520-0469(1978)035<2362:LTVODI>2.0.CO;2)
- Calvo, E., Villanueva, J., Grimalt, J. O., Boelaert, A., & Labeyrie, L. (2001). New insights into the glacial latitudinal temperature gradients in the North Atlantic. Results from UK-37 sea surface temperatures and terrigenous inputs. *Earth and Planetary Science Letters*, 188(3–4), 509–519. [https://doi.org/10.1016/S0012-821X\(01\)00316-8](https://doi.org/10.1016/S0012-821X(01)00316-8)
- Crowley, T. J. (1992). North Atlantic deep water cools the southern hemisphere. *Paleoceanography*, 7(4), 489–497. <https://doi.org/10.1029/92PA01058>
- de Vargas, C., Renaud, S., Hilbrecht, H., & Pawlowski, J. (2001). Pleistocene adaptive radiation in *Globorotalia truncatulinoides*: Genetic, morphologic, and environmental evidence. *Paleobiology*, 27(1), 104–125. [https://doi.org/10.1666/0094-8373\(2001\)027<0104:PARIGT>2.0.CO;2](https://doi.org/10.1666/0094-8373(2001)027<0104:PARIGT>2.0.CO;2)
- Dyez, K. A., Zahn, R., & Hall, I. R. (2014). Multicentennial Agulhas leakage variability and links to North Atlantic climate during the past 80,000-years. *Paleoceanography*, 29(12), 1238–1248. <https://doi.org/10.1002/2014PA002698>
- Garzoli, S. L., Baringer, M. O., Dong, S., Perez, R. C., & Yao, Q. (2013). South Atlantic meridional fluxes. *Deep Sea Research Part I: Oceanographic Research Papers*, 71, 21–32. <https://doi.org/10.1016/j.dsr.2012.09.003>
- Garzoli, S. L., & Matano, R. (2011). The South Atlantic and the Atlantic meridional overturning circulation. *Deep Sea Research Part II: Topical Studies in Oceanography*, 58(17–18), 1837–1847. <https://doi.org/10.1016/j.dsr2.2010.10.063>
- Gianelli, I., Ortega, L., Marín, Y., Piola, A., & Defeo, O. (2019). Evidence of ocean warming in Uruguay’s fisheries landings: The mean temperature of the catch approach. *Marine Ecology Progress Series*, 625, 115–125. <https://doi.org/10.3354/meps13035>
- Gottschalk, J., Skinner, L. C., & Waelbroeck, C. (2015). Contribution of seasonal sub-Antarctic surface water variability to millennial-scale changes in atmospheric CO<sub>2</sub> over the last deglaciation and Marine Isotope Stage 3. *Earth and Planetary Science Letters*, 411, 87–99. <https://doi.org/10.1016/j.epsl.2014.11.051>
- Gray, W. R., de Lavergne, C., Jnglin Wills, R. C., Menviel, L., Spence, P., Holzer, M., et al. (2023). Poleward shift in the southern hemisphere westerly winds synchronous with the deglacial rise in CO<sub>2</sub>. *Paleoceanography and Paleoclimatology*, 38(7), e2023PA004666. <https://doi.org/10.1029/2023PA004666>
- Gray, W. R., Wills, R. C. J., Rae, J. W. B., Burke, A., Ivanovic, R. F., Roberts, W. H. G., et al. (2020). Wind-driven evolution of the north pacific subpolar gyre over the Last Deglaciation. *Geophysical Research Letters*, 47(6), e2019GL086328. <https://doi.org/10.1029/2019GL086328>
- Heinrich, H. (1988). Origin and consequences of cyclic ice rafting in the Northeast Atlantic Ocean during the past 130,000 years. *Quaternary Research*, 29(2), 142–152. [https://doi.org/10.1016/0033-5894\(88\)90057-9](https://doi.org/10.1016/0033-5894(88)90057-9)
- Hüls, M., & Zahn, R. (2000). Millennial-scale sea surface temperature variability in the western tropical North Atlantic from planktonic foraminiferal census counts. *Paleoceanography*, 15(6), 659–678. <https://doi.org/10.1029/1999pa000462>
- Jonkers, L., Mix, A., Voelker, A., Risebrobakken, B., Smart, C. W., Ivanova, E., et al. (2024). ForCenS-LGM: A dataset of planktonic foraminifera species assemblage composition for the Last Glacial Maximum. *Scientific Data*, 11(1), 361. <https://doi.org/10.1038/s41597-024-03166-7>
- Kageyama, M., Albani, S., Braconnot, P., Harrison, S. P., Hopcroft, P. O., Ivanovic, R. F., et al. (2017). The PMIP4 contribution to CMIP6 – Part 4: Scientific objectives and experimental design of the PMIP4-CMIP6 Last Glacial Maximum experiments and PMIP4 sensitivity experiments. *Geoscientific Model Development*, 10(11), 4035–4055. <https://doi.org/10.5194/gmd-10-4035-2017>
- Kiefer, T. (1998). *Produktivität und Temperaturen im subtropischen Nordatlantik: Zyklische und abrupte Veränderungen im späten Quartär*, Rep. 90. Inst. Univ. Kiel.
- Köhler, P., Nehrass-Ahles, C., Schmitt, J., Stocker, T. F., & Fischer, H. (2017). A 156 kyr smoothed history of the atmospheric greenhouse gases CO<sub>2</sub>, CH<sub>4</sub>, and N<sub>2</sub>O and their radiative forcing. *Earth System Science Data*, 9(1), 363–387. <https://doi.org/10.5194/essd-9-363-2017>
- Lherminier, P., Mercier, H., Huck, T., Gourcuff, C., Perez, F. F., Morin, P., et al. (2010). The Atlantic meridional overturning circulation and the subpolar gyre observed at the A25-OVIDE section in June 2002 and 2004. *Deep Sea Research Part I: Oceanographic Research Papers*, 57(11), 1374–1391. <https://doi.org/10.1016/j.dsr.2010.07.009>
- Li, J., Roughan, M., & Kerry, C. (2022). Drivers of ocean warming in the western boundary currents of the Southern Hemisphere. *Nature Climate Change*, 12(10), 901–909. <https://doi.org/10.1038/s41558-022-01473-8>

- Lippold, J., Gutjahr, M., Blaser, P., Christner, E., de Carvalho Ferreira, M. L., Mulitza, S., et al. (2016). Deep water provenance and dynamics of the (de)glacial Atlantic meridional overturning circulation. *Earth and Planetary Science Letters*, 445, 68–78. <https://doi.org/10.1016/j.epsl.2016.04.013>
- Locarnini, R. A., Mishonov, A. V., Baranova, O. K., Boyer, T. P., Zweng, M. M., Garcia, H. E., et al. (2019). World Ocean Atlas 2018, Volume 1: Temperature NOAA Atlas NESDIS 81 (p. 52).
- Lohmann, G. P., & Schweitzer, P. N. (1990). Globorotalia truncatulinoides' Growth and chemistry as probes of the past thermocline: 1. Shell size. *Paleoceanography*, 5(1), 55–75. <https://doi.org/10.1029/pa005i001p00055>
- McManus, J. F., Francois, R., Gherardl, J. M., Kelgwin, L., & Drown-Leger, S. (2004). Collapse and rapid resumption of Atlantic meridional circulation linked to deglacial climate changes. *Nature*, 428(6985), 834–837. <https://doi.org/10.1038/nature02494>
- Mulitza, S., Dürkoop, A., Hale, W., Wefer, G., & Niebler, H. S. (1997). Planktonic foraminifera as recorders of past surface-water stratification. *Geology*, 25(4), 335–338. [https://doi.org/10.1130/0091-7613\(1997\)025<0335:pfarop>2.3.co;2](https://doi.org/10.1130/0091-7613(1997)025<0335:pfarop>2.3.co;2)
- Munk, W. H. (1950). On the wind-driven ocean circulation. *Journal of Meteorology*, 7(2), 80–93. [https://doi.org/10.1175/1520-0469\(1950\)007<0080:otwdoc>2.0.co;2](https://doi.org/10.1175/1520-0469(1950)007<0080:otwdoc>2.0.co;2)
- Pedro, J. B., Jochum, M., Buizert, C., He, F., Barker, S., & Rasmussen, S. O. (2018). Beyond the bipolar seesaw: Toward a process understanding of interhemispheric coupling. *Quaternary Science Reviews*, 192, 27–46. <https://doi.org/10.1016/j.quascirev.2018.05.005>
- Peeters, F. J. C., Acheson, R., Brummer, G. J. A., De Ruijter, W. P. M., Schneider, R. R., Ganssen, G. M., et al. (2004). Vigorous exchange between the Indian and Atlantic oceans at the end of the past five glacial periods. *Nature*, 430(7000), 661–665. <https://doi.org/10.1038/nature02785>
- Pershing, A. J., Alexander, M. A., Hernandez, C. M., Kerr, L. A., Le Bris, A., Mills, K. E., et al. (2015). Slow adaptation in the face of rapid warming leads to collapse of the Gulf of Maine cod fishery. *Science*, 350(6262), 809–812. <https://doi.org/10.1126/science.aac9819>
- Pinho, T. M. L., Chiessi, C. M., Portilho-Ramos, R. C., Campos, M. C., Crivellari, S., Nascimento, R. A., et al. (2021). Meridional changes in the South Atlantic Subtropical Gyre during Heinrich Stadials. *Scientific Reports*, 11(1), 9419. <https://doi.org/10.1038/s41598-021-88817-0>
- Primeau, F., & Cessi, P. (2001). Coupling between wind-driven currents and midlatitude storm tracks. *Journal of Climate*, 14(6), 1243–1261. [https://doi.org/10.1175/1520-0442\(2001\)014<1243:CBWDCA>2.0.CO;2](https://doi.org/10.1175/1520-0442(2001)014<1243:CBWDCA>2.0.CO;2)
- Quillévéré, F., Morard, R., Escarguel, G., Douady, C. J., Ujiie, Y., de Garidel-Thoron, T., & de Vargas, C. (2013). Global scale same-specimen morpho-genetic analysis of Truncorotalia truncatulinoides: A perspective on the morphological species concept in planktonic foraminifera. *Palaeogeography, Palaeoclimatology, Palaeoecology*, 391, 2–12. <https://doi.org/10.1016/j.palaeo.2011.03.013>
- Rainsley, E., Menviel, L., Fogwill, C. J., Turney, C. S. M., Hughes, A. L. C., & Rood, D. H. (2018). Greenland ice mass loss during the Younger Dryas driven by Atlantic Meridional Overturning Circulation feedbacks. *Scientific Reports*, 8(1), 11307. <https://doi.org/10.1038/s41598-018-29226-8>
- Reiðig, S., Nürnberg, D., Bahr, A., Poggemann, D. W., & Hoffmann, J. (2019). Southward displacement of the North Atlantic subtropical gyre circulation system during North Atlantic Cold Spells. *Paleoceanography and Paleoclimatology*, 34(5), 866–885. <https://doi.org/10.1029/2018PA003376>
- Repschläger, J., Weinelt, M., Kinkel, H., Andersen, N., Garbe-Schönberg, D., & Schwab, C. (2015). Response of the subtropical North Atlantic surface hydrography on deglacial and Holocene AMOC changes. *Paleoceanography*, 30(5), 456–476. <https://doi.org/10.1002/2014PA002637>
- Repschläger, J., Weinelt, M., Schneider, R., Blanz, T., Leduc, G., Schiebel, R., & Haug, G. H. (2023). Disentangling multiproxy temperature reconstructions from the subtropical North Atlantic. *Frontiers in Ecology and Evolution*, 11. <https://doi.org/10.3389/fevo.2023.1176278>
- Salgueiro, E., Voelker, A. H. L., de Abreu, L., Abrantes, F., Meggers, H., & Wefer, G. (2010). Temperature and productivity changes off the western Iberian margin during the last 150 ky. *Quaternary Science Reviews*, 29(5–6), 680–695. <https://doi.org/10.1016/j.quascirev.2009.11.013>
- Santos, T. P., Shimizu, M. H., Nascimento, R. A., Venancio, I. M., Campos, M. C., Portilho-Ramos, R. C., et al. (2022). A data-model perspective on the Brazilian margin surface warming from the Last Glacial Maximum to the Holocene. *Quaternary Science Reviews*, 286, 107557. <https://doi.org/10.1016/j.quascirev.2022.107557>
- Schiebel, R., Schmuker, B., Alves, M., & Hemleben, C. (2002). Tracking the Recent and late Pleistocene Azores front by the distribution of planktic foraminifera. *Journal of Marine Systems*, 37(1–3), 213–227. [https://doi.org/10.1016/S0924-7963\(02\)00203-8](https://doi.org/10.1016/S0924-7963(02)00203-8)
- Schmitz, W. J., & McCartney, M. S. (1993). On the North Atlantic Circulation. *Reviews of Geophysics*, 31(1), 29–49. <https://doi.org/10.1029/92rg02583>
- Schott, F. A., Zantopp, R., Stramma, L., Dengler, M., Fischer, J., & Wibaux, M. (2004). Circulation and deep-water export at the western exit of the subpolar North Atlantic. *Journal of Physical Oceanography*, 34(4), 817–843. [https://doi.org/10.1175/1520-0485\(2004\)034<0817:CADEAT>2.0.CO;2](https://doi.org/10.1175/1520-0485(2004)034<0817:CADEAT>2.0.CO;2)
- Shaw, T. A. (2019). Mechanisms of future predicted changes in the zonal mean mid-latitude circulation. *Current Climate Change Reports*, 5(4), 345–357. <https://doi.org/10.1007/s40641-019-00145-8>
- Shi, X., Lohmann, G., Sidorenko, D., & Yang, H. (2020). Early-Holocene simulations using different forcings and resolutions in AWI-ESM. *The Holocene*, 30(7), 996–1015. <https://doi.org/10.1177/0959683620908634>
- Shi, X., Werner, M., Yang, H., D'Agostino, R., Liu, J., Yang, C., & Lohmann, G. (2023). Unraveling the complexities of the Last Glacial Maximum climate: The role of individual boundary conditions and forcings. *The Climate of the Past*, 19(11), 2157–2175. <https://doi.org/10.5194/cp-19-2157-2023>
- Shu, Q., Wang, Q., Årthun, M., Wang, S., Song, Z., Zhang, M., & Qiao, F. (2022). Arctic Ocean Amplification in a warming climate in CMIP6 models. *Science Advances*, 8(30). <https://doi.org/10.1126/sciadv.abn9755>
- Siccha, M., & Kucera, M. (2017a). ForCenS, a curated database of planktonic foraminifera census counts in marine surface sediment samples. *Scientific Data*, 4(1), 170109. <https://doi.org/10.1038/sdata.2017.109>
- Siccha, M., & Kucera, M. (2017b). Compilation of planktonic foraminifera census counts in marine surface sediment samples (ForCenS) [Dataset]. *PANGAEA*. <https://doi.org/10.1594/PANGAEA.873570>
- Sidorenko, D., Goessling, H. F., Koldunov, N. V., Scholz, P., Danilov, S., Barbi, D., et al. (2019). Evaluation of FESOM2.0 coupled to ECHAM6.3: Preindustrial and HighResMIP simulations. *Journal of Advances in Modeling Earth Systems*, 11(11), 3794–3815. <https://doi.org/10.1029/2019MS001696>
- Steinacher, M., Joos, F., Frölicher, T. L., Bopp, L., Cadule, P., Cocco, V., et al. (2010). Projected 21st century decrease in marine productivity: A multi-model analysis. *Biogeosciences*, 7(3), 979–1005. <https://doi.org/10.5194/bg-7-979-2010>
- Stocker, T. F., & Johnsen, S. J. (2003). A minimum thermodynamic model for the bipolar seesaw. *Paleoceanography*, 18(4). <https://doi.org/10.1029/2003PA000920>
- Stramma, L., & England, M. (1999). On the water masses and mean circulation of the South Atlantic Ocean. *Journal of Geophysical Research*, 104(C9), 20863–20883. <https://doi.org/10.1029/1999JC900139>

- Stramma, L., Johnson, G. C., Sprintall, J., & Mohrholz, V. (2008). Expanding oxygen-minimum zones in the tropical oceans. *Science*, 320(5876), 655–658. <https://doi.org/10.1126/science.1153847>
- Talley, L. D. (2003). Shallow, intermediate, and deep overturning components of the global heat budget. *Journal of Physical Oceanography*, 33(3), 530–560. [https://doi.org/10.1175/1520-0485\(2003\)033<0530:SIADOC>2.0.CO;2](https://doi.org/10.1175/1520-0485(2003)033<0530:SIADOC>2.0.CO;2)
- Ujiié, Y., de Garidel-Thoron, T., Watanabe, S., Wiebe, P., & de Vargas, C. (2010). Coiling dimorphism within a genetic type of the planktonic foraminifer *Globorotalia truncatulinoides*. *Marine Micropaleontology*, 77(3–4), 145–153. <https://doi.org/10.1016/j.marmicro.2010.09.000>
- Voelker, A. H. L., & de Abreu, L. (2010). *A review of abrupt climate change events in the Northeastern Atlantic Ocean (Iberian Margin): Latitudinal, longitudinal and vertical gradients*. AGU Geophysical Monograph.
- Wang, Q., Shu, Q., Bozec, A., Chassignet, E. P., Fogli, P. G., Fox-Kemper, B., et al. (2024). Impact of increased resolution on Arctic Ocean simulations in Ocean Model Intercomparison Project phase 2 (OMIP-2). *Geoscientific Model Development*, 17(1), 347–379. <https://doi.org/10.5194/gmd-17-347-2024>
- Wu, L., Cai, W., Zhang, L., Nakamura, H., Timmermann, A., Joyce, T., et al. (2012). Enhanced warming over the global subtropical western boundary currents. *Nature Climate Change*, 2(3), 161–166. <https://doi.org/10.1038/nclimate1353>
- Yang, H., Lohmann, G., Krebs-Kanzow, U., Ionita, M., Shi, X., Sidorenko, D., et al. (2020). Poleward shift of the major ocean gyres detected in a warming climate. *Geophysical Research Letters*, 47(5). <https://doi.org/10.1029/2019GL085868>
- Yang, H., Lohmann, G., Lu, J., Gowan, E. J., Shi, X., Liu, J., & Wang, Q. (2020). Tropical expansion driven by poleward advancing midlatitude meridional temperature gradients. *Journal of Geophysical Research: Atmospheres*, 125(16). <https://doi.org/10.1029/2020JD033158>
- Yang, H., Lohmann, G., Wei, W., Dima, M., Ionita, M., & Liu, J. (2016). Intensification and poleward shift of subtropical western boundary currents in a warming climate. *Journal of Geophysical Research: Oceans*, 121(7), 4928–4945. <https://doi.org/10.1002/2015JC011513>
- Yang, H., Lu, J., Wang, Q., Shi, X., & Lohmann, G. (2022). Decoding the dynamics of poleward shifting climate zones using aqua-planet model simulations. *Climate Dynamics*, 58(11–12), 3513–3526. <https://doi.org/10.1007/s00382-021-06112-0>
- Yin, J., & Goddard, P. B. (2013). Oceanic control of sea level rise patterns along the East Coast of the United States. *Geophysical Research Letters*, 40(20), 5514–5520. <https://doi.org/10.1002/2013GL057992>

## References From the Supporting Information

- Darling, K. F., & Wade, C. M. (2008). The genetic diversity of planktic foraminifera and the global distribution of ribosomal RNA genotypes. *Marine Micropaleontology*, 67(3–4), 216–238. <https://doi.org/10.1016/j.marmicro.2008.01.009>
- Rabiner, L. R. (1989). A tutorial on hidden Markov models and selected applications in speech recognition. *Proceedings of the IEEE*, 77(2), 257–286. <https://doi.org/10.1109/5.18626>
- Renaud, S., & Schmidt, D. N. (2003). Habitat tracking as a response of the planktic foraminifer *Globorotalia truncatulinoides* to environmental fluctuations during the last 140 kyr. *Marine Micropaleontology*, 49(1–2), 97–122. [https://doi.org/10.1016/S0377-8398\(03\)00031-8](https://doi.org/10.1016/S0377-8398(03)00031-8)
- Schiebel, R., & Hemleben, C. (2017). *Planktic Foraminifers in the Modern Ocean*. Springer Berlin Heidelberg. <https://doi.org/10.1007/978-3-662-50297-6>
- Truong, C., Oudre, L., & Vayatis, N. (2020). Selective review of offline change point detection methods. *Signal Processing*, 167, 107299. <https://doi.org/10.1016/j.sigpro.2019.107299>